

Advanced glycation end products inhibit the osteogenic differentiation potential of adipose-derived stem cells in mice through autophagy

Ting Fu

The Affiliated Stomatological Hospital of Southwest Medical University

Fangzhi Lou

The Affiliated Stomatological Hospital of Southwest Medical University

Qiang Zhu

The Affiliated Stomatological Hospital of Southwest Medical University

Shuyu Cai

The Affiliated Stomatological Hospital of Southwest Medical University

Shuanglin Peng

The Affiliated Stomatological Hospital of Southwest Medical University

Jingang Xiao (✉ drxiaojiangang@163.com)

The Affiliated Stomatological Hospital of Southwest Medical University

Research Article

Keywords: Advanced glycation end products, Adipose-derived stem cells, Autophagy, Osteogenic potential

Posted Date: October 28th, 2022

DOI: <https://doi.org/10.21203/rs.3.rs-2201924/v1>

License: © ⓘ This work is licensed under a Creative Commons Attribution 4.0 International License.

[Read Full License](#)

Abstract

Diabetes microenvironment will accelerate the accumulation of Advanced glycation end products (AGEs), therefore, AGEs are a signature product in the study of the diabetes microenvironment. Adipose-derived stem cells (ASCs) have poor osteogenesis in the diabetes microenvironment, but the mechanism of the altered osteogenic potential of ASCs has not been elucidated. Bone tissue engineering by ASCs is widely used in the treatment of bone defects with diabetic osteoporosis. Therefore, this study investigated the effects of AGEs on osteogenic differentiation potential of ASCs and the underlying mechanisms. In the present study, we isolated and cultured ASCs in C57BL/6 mice, then treated ASCs with AGEs, the levels of autophagy and osteogenesis-related factors were decreased in the AGE-treated group. In order to verify autophagy and AGE-mediated changes in the osteogenic capacity of ASCs, we used 3-methyladenine, and rapamycin. After cotreatment with 3-methyladenine and AGEs, the levels of osteogenesis and autophagy were reduced more significantly, whereas rapamycin ameliorated the autophagy level and osteogenic differentiation potential of ASCs treated with AGEs. This study shows that AGEs can reduce the osteogenic differentiation potential of ASCs through autophagy, which may provide a reference for the treatment of bone defects with diabetes osteoporosis.

Introduction

Diabetes mellitus (DM) is a common chronic metabolic disease characterized by hyperglycemia resulting from insufficient insulin secretion or insulin resistance, and long-term hyperglycemia can increase the risk of osteoporosis [1, 2]. Patients with diabetes have increased bone fragility, and the risk of osteoporosis and bone fragility is several times that of normal individuals [3–6]. Therefore, bone reconstruction in diabetic patients has become a social problem. Bone tissue engineering is of great significance for treating bone defects and fractures, which consists of cells, scaffolds, and induction factors [7–10]. Among them, adipose-derived stem cells (ASCs) are easy to obtain in large quantities and have a good multidirectional differentiation potential, such as osteogenic, adipogenic, and angiogenic, and have become a hotspot in bone regeneration research [11–14].

Advanced glycation end products (AGEs) are a class of compounds produced by the reaction of glucose, proteins, lipids, and nucleic acids [15]. Increases in circulating glucose and oxidative stress in DM patients accelerate the production and accumulation of AGEs in tissues, serum, and cells, which affect the adaptability of tissues and functions. AGEs play a major role in diabetes complications such as diabetic osteoporosis, diabetic cardiovascular disease, and diabetic nephropathy [16–18]. AGEs reduce the proliferation and differentiation capacity of ASCs, thereby affecting their osteogenic capacity [19–21]. Additionally, AGEs accumulation directly affecting the bone microarchitecture, increasing bone fragility, and reducing mechanical strength [22, 23]. Therefore, AGEs are considered to be representative substances for the study of DM, but the molecular mechanism of their effect on the osteogenic potential of ASCs in the diabetes microenvironment remains unclear.

Autophagy is a process in which eukaryotic components and dysfunctional organelles are transported to lysosomes for degradation and recycling, and plays an important role in maintaining cell metabolism, internal environment stability, and genome integrity [24]. Autophagy dysfunction can lead to the pathogenesis of many human diseases such as metabolic diseases, neurodegenerative diseases, cancer, kidney diseases, and lung diseases [25]. In recent years, some studies have proposed that autophagy plays an important role in the maintenance of bone homeostasis by regulating the homeostasis of osteoblasts and osteoclasts, and participating in cell differentiation. Dysregulation of autophagy can affect bone homeostasis and lead to osteoporosis [26]. Zhang Ping proposed that insulin reduces the osteogenic ability of bone marrow stem cells (BMSCs) by inhibiting autophagy, thereby leading to bone loss in T2DM patients [27]. Moreover, AGEs cause senile osteoporosis by affecting the aging of BMSCs and inhibiting mitophagy in a concentration-dependent manner [28]. However, the role and mechanism of autophagy in the osteogenic potential of ASCs treated with AGEs have not been elucidated.

In this study, we isolated and cultured ASCs from C57BL/6 mice and explored the effects of AGEs on autophagy and osteogenesis of ASCs and the underlying molecular mechanism by analyzing changes in autophagy and osteogenesis-related molecules.

Materials Methods

Experimental animals

Four-week-old C57BL/6 mice were purchased from Chongqing Tengxin Biotechnology Co., Ltd (Chongqing, China). All animal procedures were reviewed and approved by the Ethics Committee of Southwest Medical University (20180391222). The weight of each mouse at the time of purchase was approximately 18 g. Mice have free access to drinking water and food. They were acclimatized for 1 month at a suitable temperature and humidity, and used in experiments when their weight was approximately 25–28 g.

Experimental Methods

Isolation and culture of mouse ASCs

Subcutaneous fat was harvested from the inguinal region in mice and sequentially treated with PBS containing 10% penicillin-streptomycin (Hyclone, Pittsburgh, USA), 5% penicillin-streptomycin in PBS, and PBS without penicillin-streptomycin to remove blood and hair from the tissue mass. The adipose tissue was cut into approximately 1 mm³ fragments and evenly inoculated into USA25-cm² culture flasks, each containing 4 mL modified Eagle's medium (Hyclone, Pittsburgh, USA) with 10% fetal bovine serum (Schaumburg, Pittsburgh, USA) to completely submerge the tissue blocks, followed by incubation at 37°C with 5% CO₂ for 7 days. The medium was changed every 2 days. At 80% confluence, the cells were sub-cultured, and third passage cells were used in experiments.

Characterization Of Ascs By Flow Cytometry

Passage 3 mouse ASCs were digested with 0.25% trypsin-EDTA (Gibco, New York, USA) washed three times with PBS (1000 r, 5 min), resuspended in pre-cooled PBS, and then stained with the fluorescent dye-conjugated antibodies against CD29, CD44, CD90, CD31, CD34 and CD45. An unstained sample was used as the blank control. Cells were analyzed by a flow cytometer (MoFloAstrios EQs, BECKMAN, Brea, CA, USA).

Cell Viability And Proliferation Assay

The effects of AGEs (BIOVISION, San Francisco, CA, USA), 3-methyladenine (3-MA; autophagy inhibitor, MCE), rapamycin (Rapa; autophagy agonist, MCE) on ASCs viability and proliferation were assessed and the optimal concentration was selected. Passage 3 ASCs were seeded in 96-well plates (4×10^3 cells per well), cultured for 24 hours, then treated with various concentrations of AGEs (20, 40, 60, 80, and 100 $\mu\text{g}/\text{mL}$) for 1, 4, and 7 days, 3-MA (1, 2, 3, 4, 5, 6, 7 mmol/L) for 1–3 days, or Rapa (2, 4, 6, 8, 10, 12, and 14 nmol/L) for 1, 2, and 3 days. Cell viability was assessed by CCK-8 assays. After treatment, the cells were carefully rinsed with PBS and 100 μL medium containing 10 μL CCK-8 solution was applied at 37°C for 2 hours. Optical density was measured at 450 nm using a Spectra Max M3 microplate spectrophotometer (Spectra Thermo, Switzerland). Optical density values are expressed as the average of three wells for each group. The percentage of treated cells relative to control cells was calculated as cell viability. Each experiment was repeated three times.

Western Blot Analysis

Western blotting was used to measure LC3-II/LC3-I, SQSTM1, RUNX2, and OPN levels. Treated cells were washed with PBS, and total protein was isolated from the cells using a total protein extraction kit (KEYGEN Biotech, Nanjing, China). Protein samples were mixed with loading buffer at 4:1, boiled for 10 minutes, separated by SDS-PAGE, transferred to a polyvinylidene fluoride membrane, blocked in 5% dry skim milk in Tris buffered saline with 0.05% (V/V) Tween-20 (TBST) for 1 hours, and then incubated with antibodies against GAPDH (cst5174S), LC3 (cst12741S), SQSTM1 (ab195352), RUNX2 (ab92336), or OPN (ab63856) (Abcam, Cambridge, UK) overnight at 4°C . The membrane was washed with TBST three times and then incubated with a secondary labeled anti-rabbit antibody (1:3000) for 1 h. The membrane was then washed with TBST three times and protein levels were determined using an enhanced chemiluminescence detection system (Bio-Rad, Hercules, CA, USA).

Quantitative Polymerase Chain Reaction

Quantitative polymerase chain reaction (qPCR) was used to measure mRNA expression of autophagy- and osteogenesis-related genes *Lc3*, *Sqstm1*, *Runx2*, and *Opn* in mouse ASCs after osteogenic induction. Total RNA was isolated using a total RNA extraction kit (Tiangen, Shanghai, China). A Revert Aid First

Strand cDNA synthesis kit (Thermo, Waltham, MA, USA) was used for reverse transcription into cDNA. All primers were synthesized by Sheng Gong Bioengineering Company. The specific primer sequences were as follows. *Lc3*: TTATAGAGCGATACAAGGGGGA (forward) and CGCCGTCTGATTATCTTGATGAG (reverse); *Sqstm1*: AGGAGGAGACGATGACTGGACA (forward) and TTGGTCTGTAGGAGCCTGGTGAG (reverse); *Runx2*: TCCCGTCACCTCCATCCTCTTTC (forward) and GAATACGCATCACAACAGCCACA (reverse); *Opn*: ATGGACGACGATGATGACGATGATG (forward) and CTTGTGTACTAGCAGTGACGGTC (reverse). qPCR was performed using a Prime Script RT-PCR test kit (Takara Bio, Tokyo, Japan) in a 7900 System with SDS software. Amplification and dissolution curves were determined and relative expression of target genes was calculated and statistically analyzed.

Alkaline Phosphatase (Alp) Staining

Alkaline phosphatase activity in ASCs was analyzed by alkaline phosphatase staining after treatment of ASCs with osteogenic induction medium (Cyagen, Guangzhou, China) containing AGEs, 3-MA, or Rapa. ASCs were seeded in 12-well plates at approximately 5×10^4 cells per well, and the medium was changed to osteogenic induction medium containing AGEs, 3-MA, or Rapa. The medium was changed after 3 days. After 3 and 5 days of osteogenic induction, the osteogenic induction medium was removed, and the cells were washed twice with PBS and then fixed with 4% paraformaldehyde for 30 min at 4°C. The cells were stained using an alkaline phosphatase assay kit (Beyotime, Shanghai, China), in accordance with the manufacturer's instructions to detect alkaline phosphatase activity.

Alizarin Red Staining

After incubation in osteogenic induction medium containing AGEs, 3-MA, or Rapa for 21 days, ASCs were washed twice with PBS and fixed at 4°C for 30 minutes. The cells were then stained with a 0.1% alizarin red solution at 37°C for 30 minutes to assess calcium nodule formation. Images were acquired with a camera (Canon, Tokyo, Japan).

Immunofluorescence Staining

Immunofluorescence was used to detect the expression of osteogenesis-related proteins RUNX2 and OPN after treatment with osteogenic induction medium containing AGEs, 3-MA, or Rapa. ASCs were seeded in a confocal culture dish at approximately 5×10^4 cells per dish. The cells were treated with osteogenic induction medium containing AGEs, 3-MA, or Rapa for 3 days. The cells were then fixed with 4% paraformaldehyde at 4°C for 30 minutes, treated with 0.5% Triton X-100 for 10 minutes to permeabilize the cell membrane, incubated with 5% goat serum for 1.5 hours, and then incubated with a primary antibody (1:100 dilution) against RUNX2 or OPN overnight at 4°C. The following day, the cells were rewarmed at room temperature for 30 min and then incubated with a fluorochrome-conjugated anti-rabbit secondary antibody (1:200, Invitrogen, CA, USA) for 1 h at 37°C. The cytoskeleton and nuclei of cells were

stained by incubation with FITC for 30 min and DAPI for 15 min, respectively. Cells were washed three times with PBS for 5 min between each step. Finally, images were obtained under a laser confocal microscope (Leica, Wetzlar, Germany).

Statistical analysis

Statistical analysis was conducted in SPSS 19.0 software. All experiments were repeated at least three times. The reliability of the experimental data was assessed by the t-test or one-way analysis of variance. Results are expressed as the mean \pm standard deviation (SD).

Results

Characterization of ASCs and proliferation analysis

We isolated and cultured ASCs to the third passage. The cells were spindle-shaped, plump, and evenly distributed (Fig. 1A). Flow cytometry was used to analyze cell surface antigens and the purity of ASCs. Cell surface antigens CD29, CD44, and CD90 were positive, while CD34, CD45, and CD31 were negative (Fig. 1B), which indicated high purity of the ASCs. CCK-8 assays were used to assess changes in cell proliferation and viability after AGE treatment for various times. ASC viability decreased gradually with the increase in AGE concentration and treatment time. Therefore, 80 μ g/mL AGEs were selected for subsequent experiments (Fig. 1C).

AGEs Inhibit The Osteogenic Differentiation Capacity Of ASCs

After treating ASCs in osteogenic induction medium containing AGEs for 3 days, mRNA expression levels of *Runx2* and *Opn* were measured by qPCR and protein expression levels of RUNX2 and OPN were measured by western blotting. The results of qPCR, western blotting, and immunofluorescence staining showed that, after 3 days of osteogenic induction, mRNA and protein expression levels of bone-related molecules after AGE exposure were significantly lower than in CON-ASCs (Figs. 2A, 2B, and 2D). ALP staining at 3 days showed that alkaline phosphatase in the AGE group was less than that in the CON-ASC group (Fig. 2C). After 21 days of osteogenic induction, compared with the CON-ASC group, calcium nodules formed in the AGE group were also significantly fewer (Fig. 2F). The results of qPCR, western blotting, and ALP staining after 5 days of osteogenic induction were consistent with the results at 3 days (Figs. 2E, 3A, and 3B). These results suggested that AGE treatment of ASCs inhibited their osteogenic differentiation capacity.

AGEs Inhibit Autophagy Of ASCs

After 3 days of osteogenic induction, the western blotting showed that the expression of autophagy-related molecules LC3-II/LC3-I was decreased and SQSTM1 expression was increased in the AGE group

compared with the CON group (Fig. 3A). The qPCR results were the same as the western blot results (Fig. 3B). Therefore, AGEs inhibited the autophagy process in ASCs.

Autophagy Inhibitor 3-ma Inhibits The Osteogenic Differentiation Potential Of Ascs Treated With Ages

3-MA is an inhibitor of autophagy by suppression of PI3K. We first screened the optimal concentration of 3-MA in ASCs. In accordance with the results of CCK-8 assays, we selected 5 mmol/L for experiments (Fig. 4A). After ASCs were treated with 3-MA and underwent osteogenic induction, western blotting showed that, RUNX2 and OPN expression was decreased compared with CON-ASCs, and the qPCR results were the same as western blot results (Figs. 4B, 4C, 5A, and 5B). Immunofluorescence showed that RUNX2 and OPN expression was decreased in the 3-MA group (Fig. 4D). ALP staining at 3 and 5 days of osteogenic induction showed less alkaline phosphatase in the 3-MA group than in the control group (Fig. 4E and 4F). Alizarin red staining also showed that calcium nodules were significantly reduced in the 3-MA group (Fig. 4G). More importantly, when 3-MA and AGEs acted together on ASCs, the expression of osteogenesis-related molecules was significantly lower than that after treatment with 3-MA or AGEs alone.

3-ma Inhibits Autophagy Of Ascs Treated With Ages

Subsequently, we explored the relationship between autophagy and the osteogenic differentiation potential of ASCs. After 3 days of osteogenic induction, expression of autophagy-related factors was detected. Western blotting showed that LC3-II/LC3-I expression in the 3-MA group was decreased and SQSTM1 expression was increased (Fig. 5A). The qPCR results were consistent with western blot results (Fig. 5B). These results suggested that when 3-MA acted on ASCs alone, the expression of autophagy-related molecules was consistent with the effect of AGEs. Moreover, the effect of combined treatment with AGEs and 3-MA was more pronounced than that of AGEs or 3-MA alone. These results were consistent with the changes in osteogenesis.

Rapa Rescues The Osteogenic Differentiation Potential Of Ascs Treated With Ages

To verify autophagy and AGE-mediated changes in the osteogenic capacity of ASCs, we used Rapa, an agonist of autophagy. The optimal concentration of Rapa in ASCs was 10 nmol/L (Fig. 6A). qPCR showed that *Runx2* and *Opn* expression were increased in the Rapa group, but decreased in the AGE group. *Runx2* and *Opn* expression in the AGE + Rapa group was lower than in the Rapa group, but higher than in the AGE group (Fig. 6B). Western blot results were similar to the qPCR results (Figs. 6C, 7A, and 7B). Immunofluorescence showed that RUNX2 and OPN expression was increased in the Rapa group but decreased when AGEs were applied (Fig. 6D). ALP staining showed that the content of alkaline

phosphatase was the highest in the Rapa group compared with the control group, and alkaline phosphatase was increased in the AGE + Rapa group compared with the AGEs group (Fig. 6E and 6G). Alizarin red staining at 21 days of osteogenesis revealed more calcium nodules in the Rapa group than in the AGE + Rapa group (Fig. 6F). These results suggested that Rapa rescued the reduced osteogenic capacity of ASCs caused by AGEs.

Rapa Also Rescues The Age-induced Autophagy Reduction In Ascs

We also examined the effect of Rapa on autophagy of ASCs. LC3-II/LC3-I expression was decreased and SQSTM1 expression was increased after AGE treatment, which was consistent with the above results. Conversely, Rapa treatment significantly increased LC3-II/LC3-I expression and decreased SQSTM1 expression. Additionally, in the combined AGEs and Rapa treatment group, the expression levels of LC3-II/LC3-I and SQSTM1 were between those in the AGE and Rapa groups (Fig. 7A). The qPCR results were consistent with western blot results (Fig. 7B). These results suggested that Rapamycin alleviated the effects of AGE treatment on of ASC autophagy.

Discussion

Diabetes has become a worldwide epidemic. Long-term systemic glucose metabolism disorder can lead to serious complications such as bone fractures and defects [29]. However, the current treatment methods for bone reconstruction in diabetic patients are suboptimal. Because of the reduced osteogenic potential of ASCs in the diabetic environment, bone regeneration is difficult in patients with diabetes and bone damage [30]. However, the mechanism of the reduced osteogenic differentiation potential of ASCs in the diabetic microenvironment is not fully clear. This study explored changes in osteogenesis and autophagy of ASCs in the diabetic microenvironment and the possible molecular mechanisms.

Numerous studies have shown that the formation and accumulation of AGEs are significantly increased in the diabetic microenvironment, especially in bone tissues [31–34]. Current research suggests that AGEs have a serious influence on the skeletal system. Merlo et al. found that AGE accumulation increases the brittleness of human bones and the possibility of cracks in human cortical bones by subjecting human bones in vitro to a high glucose environment [35]. In the hyperglycemic microenvironment, AGEs accumulate rapidly under the induction of glucose decomposition products, bind to their receptors, affect the expression of inflammatory factors, inhibit the proliferation of osteoblasts, increase the activity of osteoblasts, and lead to the occurrence of osteoporosis and bone fractures [36, 37]. The mechanism of the effect of AGEs on the osteogenic potential of ASCs in mice is not fully clear. In type 1 diabetes mellitus (T1DM), AGEs affect M1 macrophage polarization, leading to bone marrow mesenchymal stem cell (BMSC) dysfunction [38]. In this study, we verified the effect of AGEs on the osteogenic potential of mouse ASCs. The results showed that AGEs inhibited the proliferation of mouse ASCs in mice in a time and concentration-dependent manner, and the expression of osteogenesis-related transcription factors, such as RUNX2 and OPN, in the AGE-treated group was significantly lower than that in the CON group.

These results indicated that AGEs inhibit the osteogenic differentiation potential of ASCs in the diabetic microenvironment.

Autophagy is a highly conserved intracellular metabolic catabolism that provides cells with nutrients and energy, and controls the chemical balance of each cell [39]. It is also closely related to bone homeostasis in the context of diabetes. A recent study by Jiang et al. showed that $1\alpha,25$ -dihydroxyvitamin D₃ reduces the bone loss caused by diabetes by reducing FoxO1-mediated autophagy [40]. Chen et al. found that PPAR β/δ agonists promote the osteogenic differentiation of rBMSCs by mediating AMPK/mTOR-regulated autophagy [41]. Our study showed that LC3 expression was decreased and SQSTM1 expression was increased in the AGE-treated group. To further investigate the relationship between AGE-induced autophagy and osteogenesis, we used 3-MA, a canonical autophagy inhibitor that acts on the canonical PI3K/AKT autophagy inhibitory signaling pathway [42]. After treatment of ASCs with 3-MA, we found decreases in autophagy and osteogenesis-related factors RUNX2 and OPN. Interestingly, when we combined 3-MA and AGEs, the inhibitory effect on autophagy and osteogenesis was more pronounced. Therefore, we speculated that the effect of AGEs on autophagy and the osteogenic potential of ASCs may be the same effect as 3-MA, and autophagy was also involved in the change of the AGE-induced osteogenic potential of ASCs. To verify the mechanism of AGEs, we used Rapa that activates autophagy by inhibiting the mTOR receptor [43]. After applying Rapa, autophagy and the osteogenic ability of ASCs were increased, but when combined with AGEs, the osteogenesis and autophagy were lower than those in cells treated with Rapa alone. This indicated that the autophagy activator Rapa alleviated the inhibitory effect of AGEs on autophagy and osteogenesis of ASCs. Thus, AGEs affected the osteogenic differentiation ability of ASCs through autophagy in the diabetic microenvironment.

In conclusion, this study provides an explanation for the reduced osteogenic capacity of ASCs in the diabetic microenvironment by demonstrating that AGEs reduce the osteogenic capacity of ASCs by inhibiting autophagy. However, further studies are needed to determine the exact mechanism of AGE-mediated autophagy and osteogenesis, which may provide a possible approach for bone tissue regeneration in diabetic osteoporosis.

Declarations

Funding

This work was supported by National Natural Science Foundation of China (81870746), Project of Science & Technology Department of Sichuan Province (2022NSFSC0599), Open Project of State Key Laboratory of Oral Disease Research (SKLOD20210F08), Joint project of Luzhou Municipal People's Government and Southwest Medical University (2020LZXNYDZ09), Key Program of Southwest Medical University (2021ZKZD009), and Project of Stomatological Institute of Southwest Medical University (2021XJYJS01), Youth Research Project of Southwest Medical University (2021ZKQN031).

Competing Interests

The authors have no relevant financial or non-financial interests to disclose.

Author Contributions

All authors contributed to the study conception and design. Ting Fu conducted experiments, executed the analysis of the data, and wrote the first draft. Fangzhi Lou and Qiang zhu collected the data. Shuyu Cai raised mice and cultured ASCs. Shuanglin Peng designed the study and revised the manuscript. Jingang Xiao conceived and initiated the study, analyzed the data, and provided funding. All authors read and approved the final manuscript.

Data Availability

All data included in this article can be obtained from corresponding author upon reasonable requirements.

Ethics approval

This study was performed in line with the principles of the Declaration of Helsinki. Approval was granted by the Ethics Committee of Southwest Medical University(20180391222).

Consent to participate

Not applicable.

Consent to publish

Not applicable.

Acknowledgment

This work was supported by National Natural Science Foundation of China (81870746), Project of Science & Technology Department of Sichuan Province (2022NSFSC0599), Open Project of State Key Laboratory of Oral Disease Research (SKLOD2021OF08), Joint project of Luzhou Municipal People's Government and Southwest Medical University (2020LZXNYDZ09), Key Program of Southwest Medical University (2021ZKZD009), and Project of Stomatological Institute of Southwest Medical University (2021XJYJS01), Youth Research Project of Southwest Medical University (2021ZKQN031).

References

1. Compston J (2018) Type 2 diabetes mellitus and bone. *J Intern Med* 283(2):140–153. <https://doi.org/10.1111/joim.12725>
2. Sruthi CR, Raghu KG(2021) Advanced glycation end products and their adverse effects: The role of autophagy. *J Biochem Mol Toxicol* 35(4):e22710. <https://doi.org/10.1002/jbt.22710>

3. Zhang Z-D, Ren H, Wang W-X, et al (2019) IGF-1R/ β -catenin signaling axis is involved in type 2 diabetic osteoporosis. *J Zhejiang Univ Sci B* 20(10):838–848.
<https://doi.org/10.1631/jzus.B1800648>
4. Carey IM, Critchley JA, DeWilde S, Harris T, Hosking FJ, Cook DG (2018) Risk of Infection in Type 1 and Type 2 Diabetes Compared With the General Population: A Matched Cohort Study. *Diabetes Care* 41(3):513–521. <https://doi.org/10.2337/dc17-2131>
5. Hunt HB, Miller NA, Hemmerling KJ, et al(2021) Bone Tissue Composition in Postmenopausal Women Varies With Glycemic Control From Normal Glucose Tolerance to Type 2 Diabetes Mellitus. *J Bone Miner Res* 36(2):334–346. <https://doi.org/10.1002/jbmr.4186>
6. Mitchell A, Fall T, Melhus H, Lind L, Michaëlsson K, Byberg L (2021) Type 2 Diabetes and Change in Total Hip Bone Area and Bone Mineral Density in Swedish Men and Women Older Than 55 Years. *J Clin Endocrinol Metab* 106(10):2840–2854. <https://doi.org/10.1210/clinem/dgab490>
7. Agarwal R, García AJ (2015) Biomaterial strategies for engineering implants for enhanced osseointegration and bone repair. *Adv Drug Deliv Rev* 94:53–62.
<https://doi.org/10.1016/j.addr.2015.03.013>
8. Liao J, Tian T, Shi S, et al (2017). The fabrication of biomimetic biphasic CAN-PAC hydrogel with a seamless interfacial layer applied in osteochondral defect repair. *Bone research*, 5, 17018.
<https://doi.org/10.1038/boneres.2017.18>
9. Zhang Q-Y, Huang K, Tan J, et al(2022). Zhang, Qingyi; Huang, Kai; Tan, Jie; Lei, Xiongxin; Huang, Liping; Song, Yuting; Li, Qianjin; Zou, Chenyu; Xie, Huiqi. *Chin. Chem. Lett.*, 33 (3): 1623–1626.
<https://doi.org/10.1016/j.ccllet.2021.09.105>
10. Wang L-L, Chen L, Wang J-P, et al(2022). Bioactive gelatin cryogels with BMP-2 biomimetic peptide and VEGF: A potential scaffold for synergistically induced osteogenesis. *Chin. Chem. Lett.*, 33 (4): 1956–1962. <https://doi.org/10.1016/j.ccllet.2021.10.070>
11. Cheng T-Y, Xiao D-X, Li Y-J, et al(2022). Tetrahedral framework nucleic acids regulate osteogenic differentiation potential of osteoporotic adipose-derived stem cells. *Chin. Chem. Lett.*, 33 (5): 2517–2521. <https://doi.org/10.1016/j.ccllet.2021.11.090>
12. Dai R, Wang Z, Samanipour R, Koo KI, Kim K (2016) Adipose-Derived Stem Cells for Tissue Engineering and Regenerative Medicine Applications. *Stem Cells Int* 2016:6737345.
<https://doi.org/10.1155/2016/6737345>
13. Fennema EM, Tchang LAH, Yuan H, et al (2018) Ectopic bone formation by aggregated mesenchymal stem cells from bone marrow and adipose tissue: A comparative study. *J Tissue Eng Regen Med* 12(1):e150-e158. <https://doi.org/10.1002/term.2453>
14. Wang G, Roohani-Esfahani SI, Zhang W, et al (2017) Effects of Sr-HT-Gahnite on osteogenesis and angiogenesis by adipose derived stem cells for critical-sized calvarial defect repair. *Sci Rep* 7:41135.
<https://doi.org/10.1038/srep41135>
15. Xie X, Yang C, Duan C, et al (2020) Advanced glycation end products reduce macrophage-mediated killing of *Staphylococcus aureus* by ARL8 upregulation and inhibition of autolysosome formation.

- Eur J Immunol 50(8):1174–1186. <https://doi.org/10.1002/eji.201948477>
16. Perrone A, Giovino A, Benny J, et al (2020) Advanced Glycation End Products (AGEs): Biochemistry, Signaling, Analytical Methods, and Epigenetic Effects. *Oxid Med Cell Longev* 2020:3818196. <https://doi.org/10.1155/2020/3818196>
 17. Yamamoto M, Sugimoto T (2016) Advanced Glycation End Products, Diabetes, and Bone Strength. *Curr Osteoporos Rep* 14(6):320–326. <https://doi.org/10.1007/s11914-016-0332-1>
 18. Gómez O, Perini-Villanueva G, Yuste A, et al (2021) Autophagy and Glycative Stress: A Bittersweet Relationship in Neurodegeneration. *Front Cell Dev Biol* 9:790479. <https://doi.org/10.3389/fcell.2021.790479>
 19. Nowotny K, Jung T, Höhn A, et al (2015) Advanced glycation end products and oxidative stress in type 2 diabetes mellitus. *Biomolecules* 5(1):194–222. <https://doi.org/10.3390/biom5010194>
 20. Yang P, Feng J, Peng Q, et al (2019) Advanced Glycation End Products: Potential Mechanism and Therapeutic Target in Cardiovascular Complications under Diabetes. *Oxid Med Cell Longev* 2019:9570616. <https://doi.org/10.1155/2019/9570616>
 21. Mattioli-Belmonte M, Teti G, Salvatore V, et al (2015) Stem cell origin differently affects bone tissue engineering strategies. *Front Physiol* 6:266. <https://doi.org/10.3389/fphys.2015.00266>
 22. Piccoli A, Cannata F, Strollo R, et al (2020) Sclerostin Regulation, Microarchitecture, and Advanced Glycation End-Products in the Bone of Elderly Women With Type 2 Diabetes. *J Bone Miner Res* 35(12):2415–2422. <https://doi.org/10.1002/jbmr.4153>
 23. Tabara Y, Ikezoe T, Yamanaka M, et al (2019) Advanced Glycation End Product Accumulation Is Associated With Low Skeletal Muscle Mass, Weak Muscle Strength, and Reduced Bone Density: The Nagahama Study. *J Gerontol A Biol Sci Med Sci* 74(9):1446–1453. <https://doi.org/10.1093/gerona/gly233>
 24. Zhang W, Han Z, Xue Y, Jia D (2021) iCAL: a new pipeline to investigate autophagy selectivity and cancer. *Autophagy* 17(7):1799–1801. <https://doi.org/10.1080/15548627.2021.1939972>
 25. Liao S-X, Sun P-P, Gu Y-H, Rao XM, Zhang LY, Ou-Yang Y (2019) Autophagy and pulmonary disease. *Ther Adv Respir Dis* 13:1753466619890538. <https://doi.org/10.1177/1753466619890538>
 26. Guo Y-F, Su T, Yang M, et al (2021) The role of autophagy in bone homeostasis. *J Cell Physiol* 236(6):4152–4173. <https://doi.org/10.1002/jcp.30111>.
 27. Zhang P, Zhang H, Lin J, et al (2020) Insulin impedes osteogenesis of BMSCs by inhibiting autophagy and promoting premature senescence via the TGF- β 1 pathway. *Aging (Albany NY)* 12(3):2084–2100. <https://doi.org/10.18632/aging.102723>.
 28. Guo Y, Jia X, Cui Y, et al (2021) Sirt3-mediated mitophagy regulates AGEs-induced BMSCs senescence and senile osteoporosis. *Redox Biol* 41:101915. <https://doi.org/10.1016/j.redox.2021.101915>
 29. Shitole P, Choubey A, Mondal P, Ghosh R (2021) Influence of low dose naltrexone on Raman assisted bone quality, skeletal advanced glycation end-products and nano-mechanical properties in type 2

- diabetic mice bone. *Mater Sci Eng C Mater Biol Appl* 123:112011.
<https://doi.org/10.1016/j.msec.2021.112011>
30. Peng S, Gao Y, Shi S, et al (2022) LncRNA-AK137033 inhibits the osteogenic potential of adipose-derived stem cells in diabetic osteoporosis by regulating Wnt signaling pathway via DNA methylation. *Cell Prolif* 55(1):e13174. <https://doi.org/10.1111/cpr.13174>
 31. Khan MY, Alouffi S, Khan MS, Husain FM, Akhter F, Ahmad S (2020) The neoepitopes on methylglyoxal (MG) glycated LDL create autoimmune response; autoimmunity detection in T2DM patients with varying disease duration. *Cell Immunol* 351:104062.
<https://doi.org/10.1016/j.cellimm.2020.104062>
 32. Le Bagge S, Fotheringham AK, Leung SS, Forbes JM (2020) Targeting the receptor for advanced glycation end products (RAGE) in type 1 diabetes. *Med Res Rev* 40(4):1200–1219.
<https://doi.org/10.1002/med.21654>
 33. Zhou L, Wang W, Yang C, et al (2018) GADD45a Promotes Active DNA Demethylation of the MMP-9 Promoter via Base Excision Repair Pathway in AGEs-Treated Keratinocytes and in Diabetic Male Rat Skin. *Endocrinology* 159(2):1172–1186. <https://doi.org/10.1210/en.2017-00686>
 34. Lekkala S, Taylor EA, Hunt HB, Donnelly E (2019) Effects of Diabetes on Bone Material Properties. *Curr Osteoporos Rep* 17(6):455–464. <https://doi.org/10.1007/s11914-019-00538-6>
 35. Merlo K, Aaronson J, Vaidya R, Rezaee T, Chalivendra V, Karim L (2020) In Vitro-Induced High Sugar Environments Deteriorate Human Cortical Bone Elastic Modulus and Fracture Toughness. *J Orthop Res* 38(5):972–983. <https://doi.org/10.1002/jor.24543>
 36. Karim L, Bouxsein ML (2016) Effect of type 2 diabetes-related non-enzymatic glycation on bone biomechanical properties. *Bone* 82:21–27. <https://doi.org/10.1016/j.bone.2015.07.028>
 37. Roy B (2013) Biomolecular basis of the role of diabetes mellitus in osteoporosis and bone fractures. *World J Diabetes* 4(4):101–113. <https://doi.org/10.4239/wjd.v4.i4.101>
 38. Wang F, Kong L, Wang W, et al(2021) Adrenomedullin 2 improves bone regeneration in type 1 diabetic rats by restoring imbalanced macrophage polarization and impaired osteogenesis. *Stem Cell Res Ther* 12(1):288. <https://doi.org/10.1186/s13287-021-02368-9>
 39. Yin X, Zhou C, Li J, et al (2019) Autophagy in bone homeostasis and the onset of osteoporosis. *Bone Res* 7:28. <https://doi.org/10.1038/s41413-019-0058-7>
 40. Jiang Y, Luo W, Wang B, et al(2021) 1 α ,25-Dihydroxyvitamin D3 ameliorates diabetes-induced bone loss by attenuating FoxO1-mediated autophagy. *J Biol Chem* 296:100287.
<https://doi.org/10.1016/j.jbc.2021.100287>
 41. Chen M, Jing D, Ye R, Yi J, Zhao Z (2021) PPAR β/δ accelerates bone regeneration in diabetic mellitus by enhancing AMPK/mTOR pathway-mediated autophagy. *Stem Cell Res Ther* 12(1):566.
<https://doi.org/10.1186/s13287-021-02628-8>
 42. Kim Y-C, Guan K-L (2015) mTOR: a pharmacologic target for autophagy regulation. *J Clin Invest* 125(1):25–32. <https://doi.org/10.1172/JCI73939>

43. Ping X, Liang J, Shi K, et al (2021) Rapamycin relieves the cataract caused by ablation of Gja8b through stimulating autophagy in zebrafish. *Autophagy* 17(11):3323–3337.
<https://doi.org/10.1080/15548627.2021.1872188>

Figures

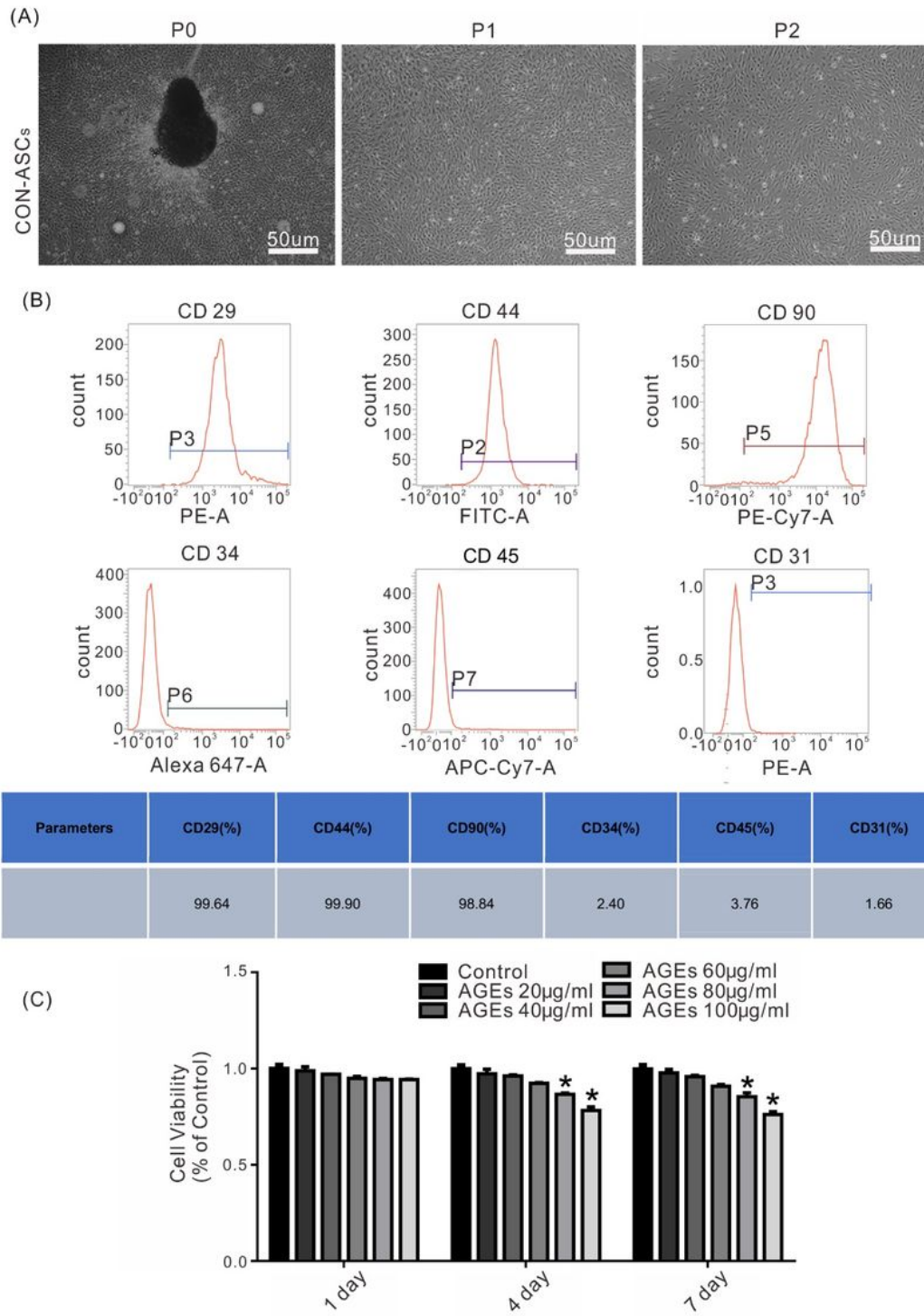


Figure 1

Isolation and culture of CON-ASCs and analysis of cell proliferation. **A**, Passage 0–2 cells under an inverted microscope, showing a spindle shape. **B**, Flow cytometric analysis of passage 3 ASC surface antigens. **C**, CCK-8 assays of the proliferative activity of ASCs treated with AGEs. The inhibitory effect on mouse ASC proliferation was enhanced in an AGE concentration-dependent manner. Data are shown as means \pm SD ($n = 3$), * $P < 0.05$, ** $P < 0.01$, *** $P < 0.001$.

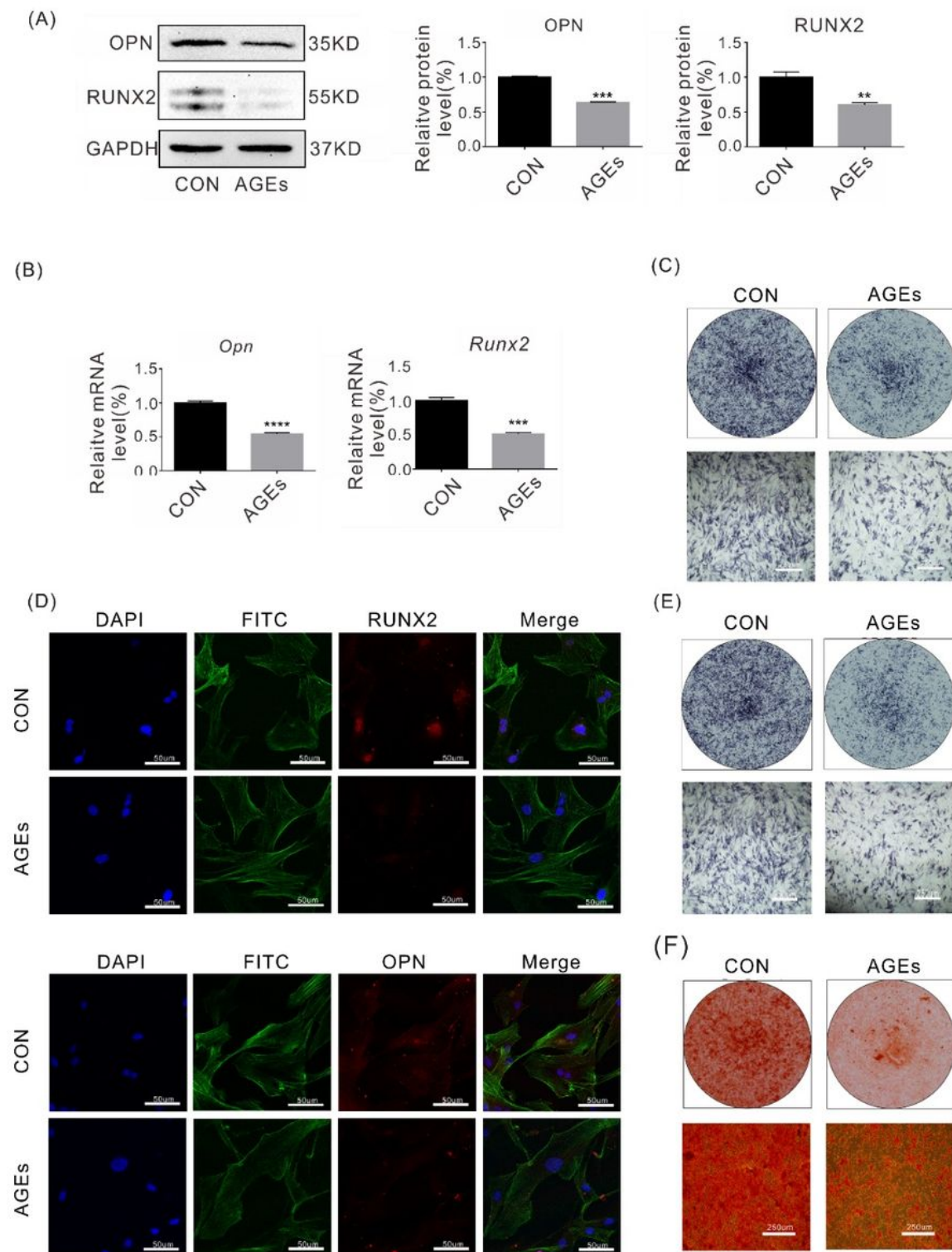


Figure 2

AGEs inhibit the osteogenic differentiation potential of ASCs. **A** Western blot analysis of RUNX2 and OPN expression in CON and AGE groups. **B** qPCR analysis of RUNX2 and OPN expression in CON and AGE groups. **C E F**, ALP and Alizarin Red staining showed decreases in alkaline phosphatase activity and fewer calcium nodules after treatment with AGEs compared the controls, respectively. **D** Immunofluorescence staining of RUNX2 and OPN proteins after 3 days of osteogenic induction.

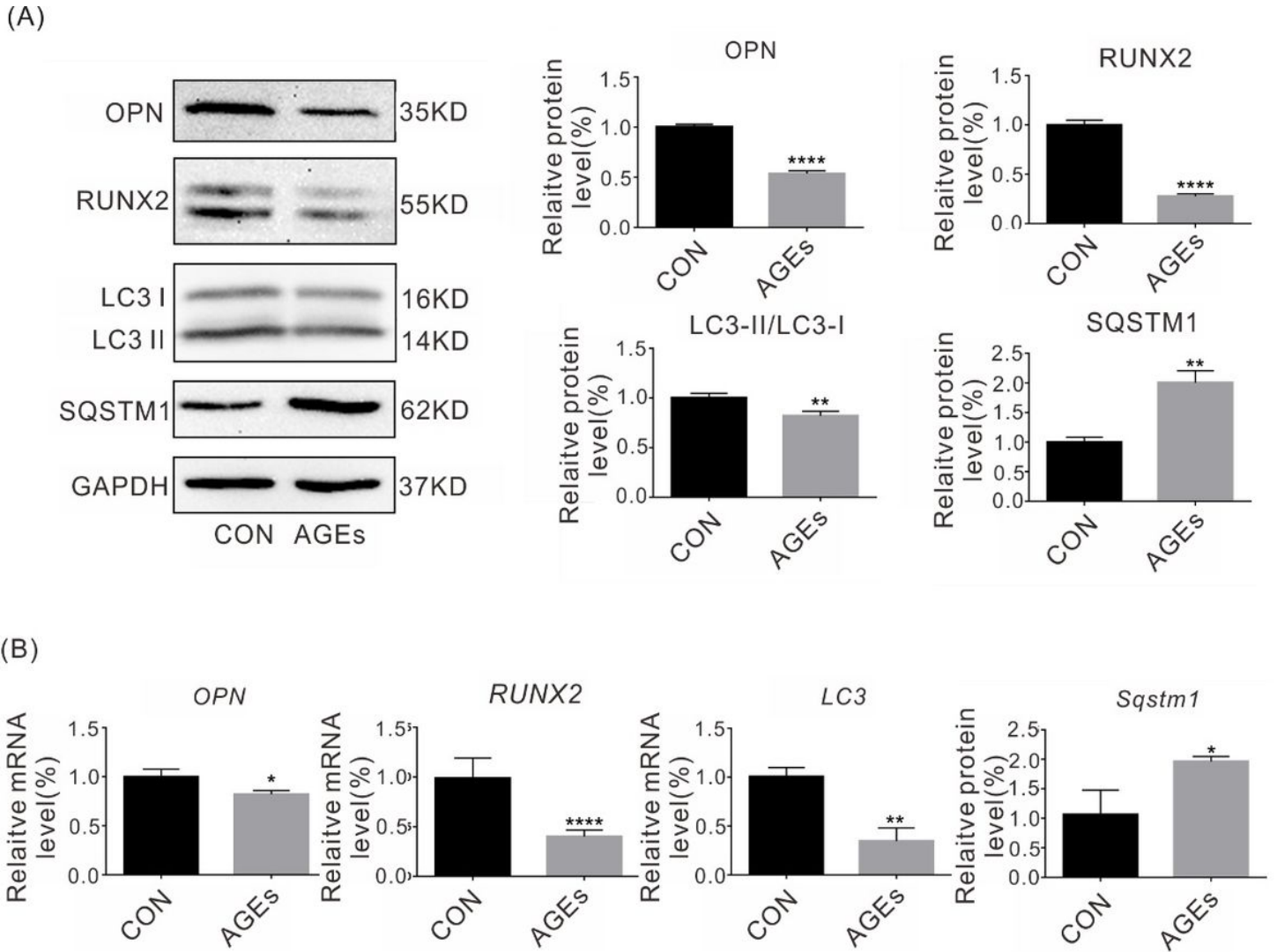


Figure 3

AGEs inhibit autophagy and osteogenesis of ASCs. **A** Western blot analysis showed that RUNX2, OPN, and LC3-II/LC3-IAGE expression was decreased, and SQSTM1 expression was increased (5 days of osteogenic induction). **B** qPCR analysis of *Runx2*, *Opn*, *Lc3*, and *Sqstm1* expression in CON and AGE groups (5 days of osteogenic induction).

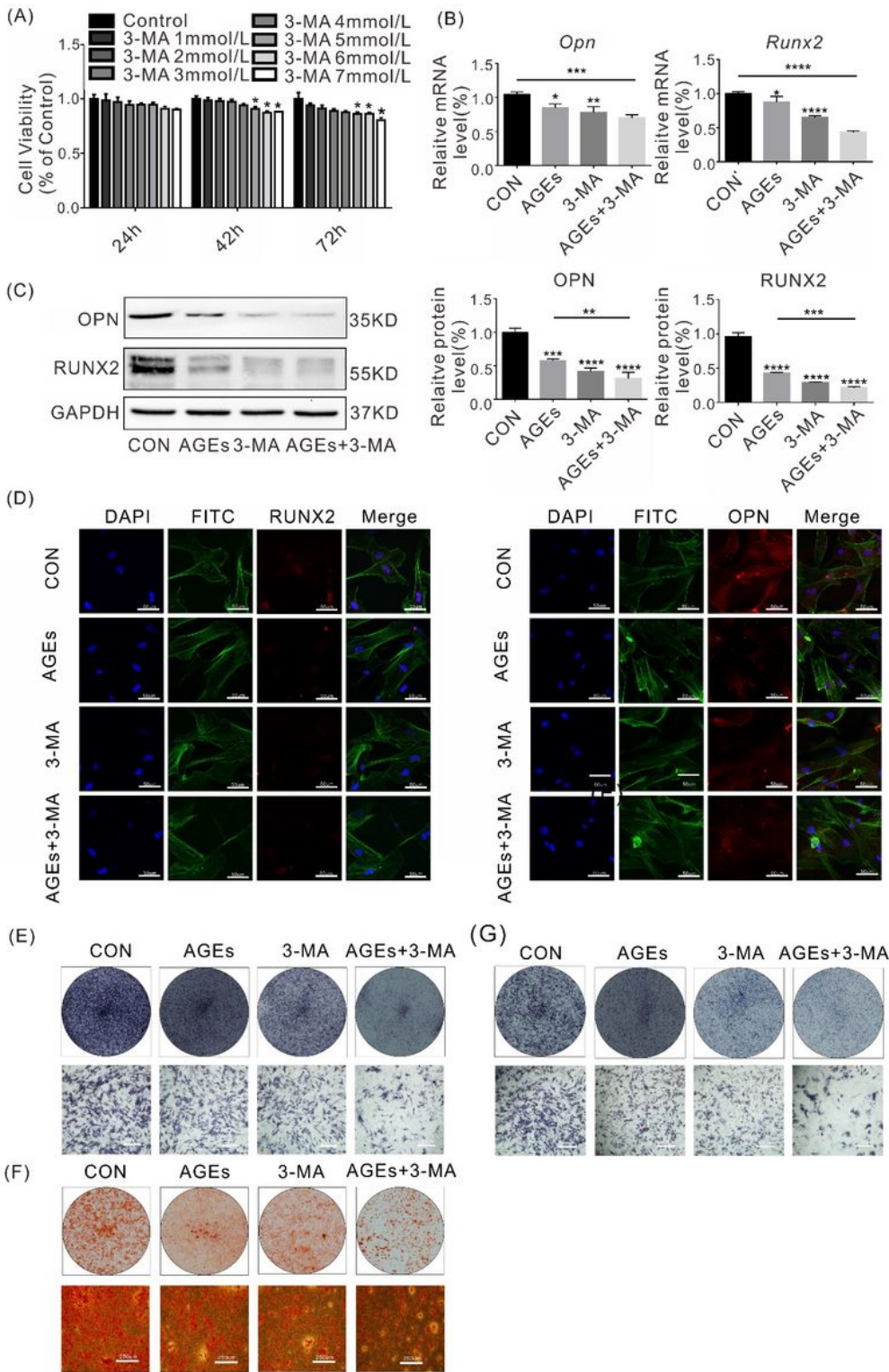


Figure 4

Both AGEs and 3-MA inhibit the osteogenic differentiation potential of mouse ASCs. **A** The inhibitory effect on mouse ASCs proliferation was enhanced in the 3-MA concentration-dependent manner. **B** after 3 days of osteogenic induction, western blot analysis showed that both AGEs and 3-MA reduced the levels of osteogenesis-related molecules RUNX2 and OPN in ASCs. **C** After 3 days of osteogenic induction, qPCR showed that both AGEs and 3-MA reduced the levels of osteogenesis-related molecules RUNX2 and

OPN in ASCs. **D** Immunofluorescence staining of RUNX2 and OPN proteins after treatment with AGEs and 3-MA compared with the control group. **E F** Osteogenesis was induced for 3 and 5 days, and ALP staining showed that both AGEs and 3-MA reduced alkaline phosphatase activity in ASCs. **G**, after 21 days of osteogenic induction, the calcium nodule content in AGE- and 3-MA-treated groups was significantly lower than that in the control group. Data are shown as means \pm SD ($n = 3$), $*P < 0.05$, $**P < 0.01$, $***P < 0.001$.

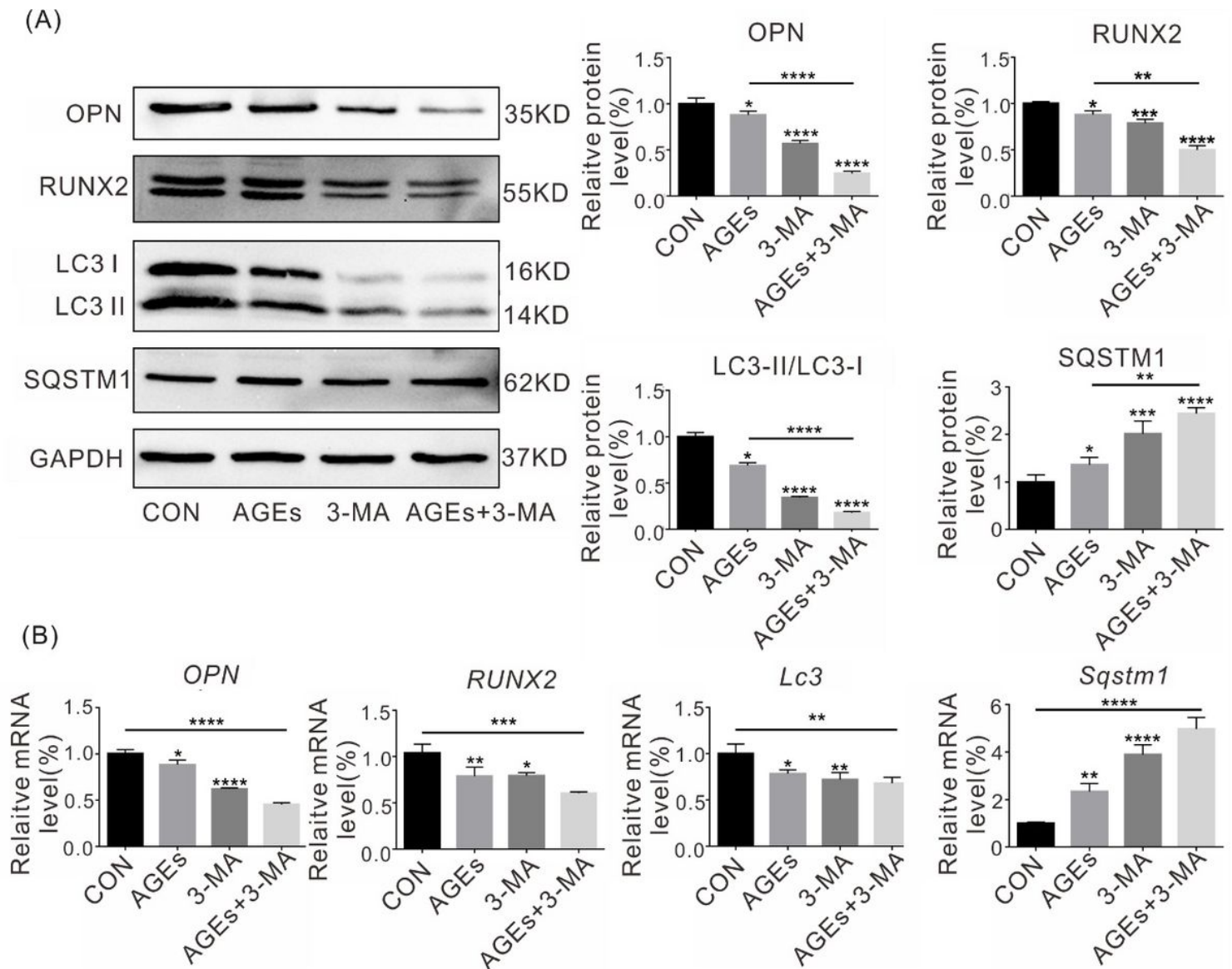


Figure 5

AGEs and 3-MA inhibit autophagy of ASCs. **A B** After AGE and 3-MA treatment of mouse ASCs, western blotting was used to measure autophagy and osteogenesis-related proteins. The results showed that autophagy and osteogenesis-related proteins LC3II/I, RUNX2, and OPN were decreased in AGE, 3-MA, and AGE+3-MA groups, while SQSTM1 expression was increased, and combined treatment with AGEs and 3-MA was significantly stronger than AGEs or 3-MA alone.

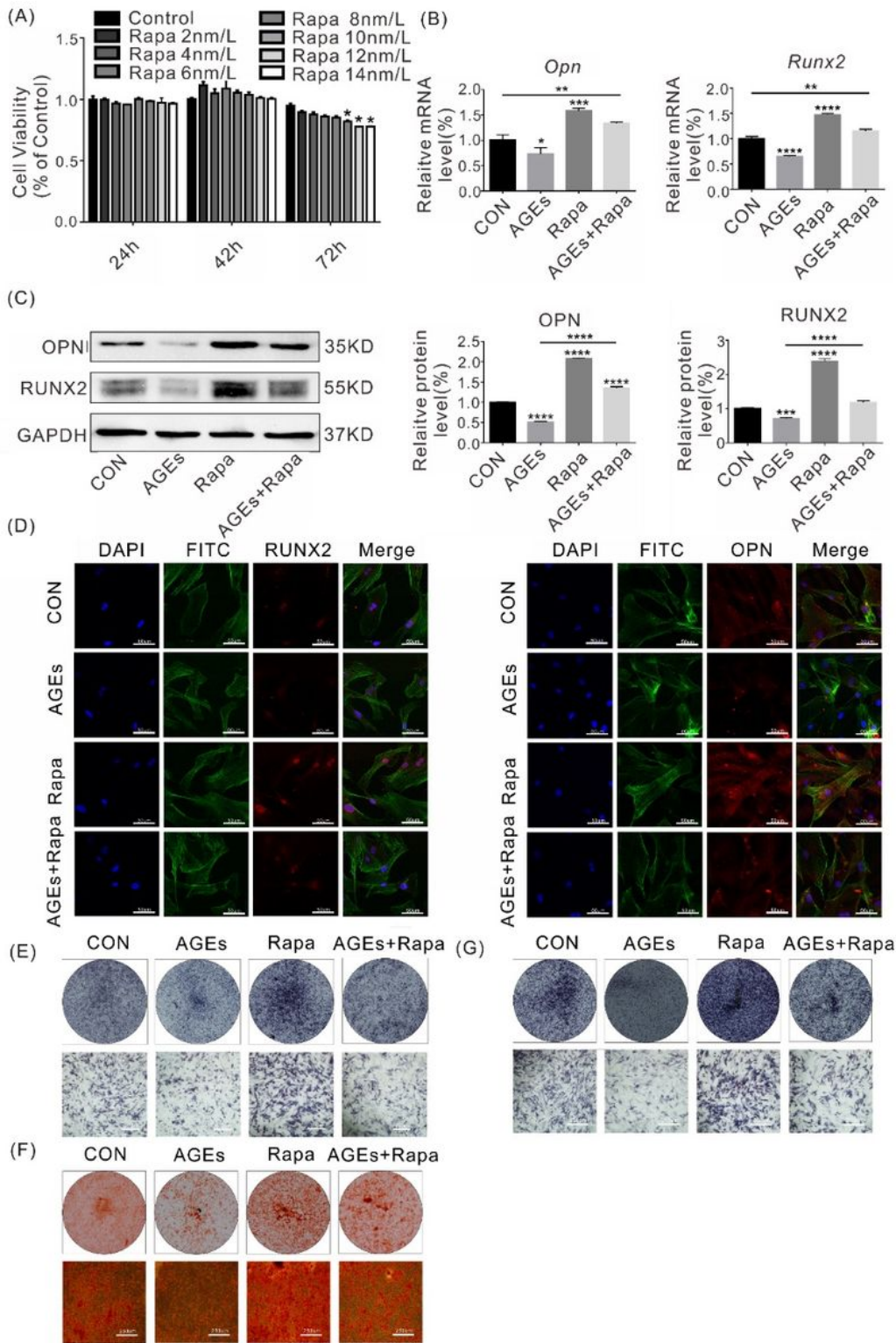


Figure 6

Rapamycin alleviates the decreased osteogenic potential of ASCs caused by AGEs. **A** Effects of rapamycin treatment on the proliferative viability of ASCs. **B C** Western blotting and qPCR showed that Rapa treatment of ASCs increased the expression of osteogenic factors RUNX2 and OPN, which alleviated the inhibitory effect of AGE treatment on ASCs. **D** Immunofluorescence staining of RUNX2 and OPN proteins after AGE and Rapa treatment (3 days of osteogenic induction). **E F** After 3 and 5 days of

osteogenic induction, ALP staining showed that AGEs decreased the alkaline phosphatase activity of ASCs, whereas Rapa significantly increased the alkaline phosphatase activity of ASCs. Compared with the Rapa group, combined treatment with AGEs and Rapa reduced alkaline phosphatase activity. G, Alizarin red staining after 21 days of osteogenic induction showed that calcium nodules were significantly reduced in the AGE group, and rapamycin rescued the reduced osteogenic differentiation ability of ASCs caused by AGEs. Data are shown as means \pm SD (n = 3), * P < 0.05, ** P < 0.01, *** P < 0.001.

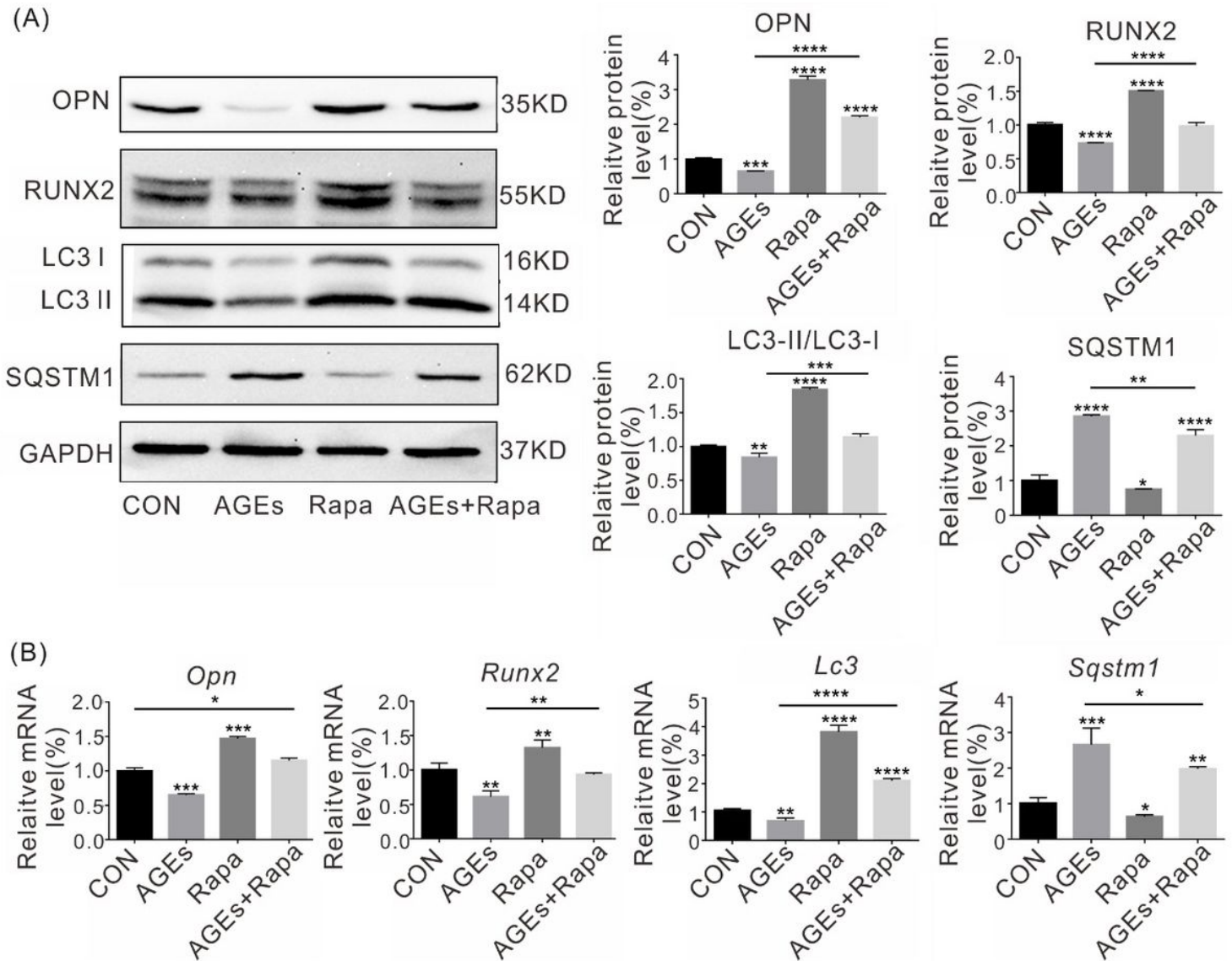


Figure 7

Rapamycin rescues the reduced osteogenic differentiation capacity of ASCs caused by AGEs by activating autophagy. **A B** after mouse ASCs were treated with AGEs and rapamycin, western blotting was used to measure autophagy and osteogenesis-related proteins. The results showed that autophagy and osteogenesis-related LC3II/I proteins and mRNA expression was decreased in the AGE group, and SQSTM1 expression was increased. Autophagy and osteogenesis-related protein and mRNA expression

was increased in the rapamycin group, while SQSTM1 expression was decreased in the rapamycin group. Autophagy and osteogenesis-related protein and mRNA expression in the AGE+Rapa group was relatively restored compared with the AGE group.